Kinetics of a Two-Component *p*-Hydroxyphenylacetate Hydroxylase Explain How Reduced Flavin Is Transferred from the Reductase to the Oxygenase†

Jeerus Sucharitakul,[‡,§] Thanawat Phongsak,[‡] Barrie Entsch,[||,⊥] Jisnuson Svasti,[‡] Pimchai Chaiyen,*[,‡] and David P. Ballou*[,||]

Department of Biochemistry and Center for Excellence in Protein Structure and Function, Faculty of Science, Mahidol University, Bangkok 10400, Thailand, Department of Biochemistry, Faculty of Dentistry, Chulalongkorn University, Henri-Dunant Road, Bangkok 10300, Thailand, Department of Biological Chemistry, University of Michigan, Ann Arbor, Michigan 48109-06060, and School of Biological, Biomedical and Molecular Sciences, University of New England, Armidale, New South Wales 2351, Australia

Received April 8, 2007; Revised Manuscript Received May 23, 2007

ABSTRACT: *p*-Hydroxyphenylacetate hydroxylase (HPAH) from *Acinetobacter baumannii* catalyzes the hydroxylation of *p*-hydroxyphenylacetate (HPA) to form 3,4-dihydroxyphenylacetate (DHPA). HPAH is composed of two proteins: a flavin mononucleotide (FMN) reductase (C_1) and an oxygenase (C_2). C_1 catalyzes the reduction of FMN by NADH to generate reduced FMN ($FMNH^-$) for use by C_2 in the hydroxylation reaction. C_1 is unique among the flavin reductases in that the substrate HPA stimulates the rates of both the reduction of FMN and release of $FMNH^-$ from the enzyme. This study quantitatively shows the kinetics of how the C_1-bound FMN can be reduced and released to be used efficiently as the substrate for the C_2 reaction; additional FMN is not necessary. Reactions in which O_2 is rapidly mixed with solutions containing C_1-FMNH^- and C_2 are very similar to those in which solutions containing O_2 are mixed with one containing the C_2-FMNH^- complex. This suggests that in a mixture of the two proteins $FMNH^-$ binds more tightly to C_2 and has already been completely transferred to C_2 before it reacts with oxygen. Rate constants for the transfer of $FMNH^-$ from C_1 to C_2 were found to be 0.35 and ≥ 74 s^{-1} in the absence and presence of HPA, respectively. The reduction of cytochrome *c* by $FMNH^-$ was also used to measure the dissociation rate of $FMNH^-$ from C_1. In the absence of HPA, $FMNH^-$ dissociates from C_1 at 0.35 s^{-1}, while with HPA present it dissociates at 80 s^{-1}; these are the same rates as those for the transfer from C_1 to C_2. Therefore, the dissociation of $FMNH^-$ from C_1 is rate-limiting in the intermolecular transfer of $FMNH^-$ from C_1 to C_2, and this process is regulated by the presence of HPA. This regulation avoids the production of H_2O_2 in the absence of HPA. Our findings indicate that no protein−protein interactions between C_1 and C_2 are necessary for efficient transfer of $FMNH^-$ between the proteins; transfer can occur by a rapid-diffusion process, with the rate-limiting step being the release of $FMNH^-$ from C_1.

In the past decade, many two-component monooxygenases have been identified and studied (*1*, *2*). The enzymes of this class, which are comprised of reductase and monooxygenase components, are involved in a wide variety of reactions, including monooxygenation of *p*-hydroxyphenylacetate (*3*−*5*), phenol (*6*, *7*), chlorophenol (*8*), 2,4,6-trichlorophenol (*9*), pyrrole-2-carboxylate (*10*), styrene (*11*, *12*), *p*-nitrophenol (*13*), nitrilotriacetate (*14*), ethylenediaminetetraacetic acid (EDTA) (*15*), alkane sulfonate (*16*), and aldehyde (bacterial luciferase) (*17*, *18*). These oxygenases are also involved in the biosynthesis of the antibiotics, actinorhodin (*19*, *20*), pristinamycin IIA (*21*), and valinomycin (*22*), as well as the halogenation in the biosynthesis of rebeccamycin (*23*, *24*).

The reductase components of these enzymes generate reduced flavin to be used in the monooxygenation reactions catalyzed by the oxygenases. The mechanism by which the reactive reduced flavin is transferred between protein components is one of the most interesting research questions in this field and is the main focus of this paper, in which *p*-hydroxyphenylacetate hydroxylase (HPAH)[1] from *Acinetobacter baumannii* was used as a model for this study.

HPAH catalyzes the hydroxylation of *p*-hydroxyphenylacetate (HPA) to form 3,4-dihydroxyphenylacetate (DHPA), and the enzyme has been identified and studied from four bacterial species; *Pseudomonas putida* (*25*, *26*), *Pseudomo-*

† This work was supported by NIH Grant GM64711 (to D.P.B.), Thailand Research Fund Grants RMU4880028 and RTA4780006, and a grant from the Faculty of Science, Mahidol University (to P.C.). J.S. was a recipient of a scholarship under the Commission on Higher Education Staff Development Project, Chulalongkorn University. T.P. is a recipient of a CHE-PhD-SW-INV scholarship from the Commission on Higher Education, Thailand. This study was also partly supported by a Research Team Strengthening Grant from BIOTECH to Skorn Mongkolsuk.

* To whom correspondence should be addressed: Department of Biochemistry and Center for Excellence in Protein Structure and Function, Faculty of Science, Mahidol University, Rama 6 Road, Bangkok 10400, Thailand. Telephone: 662-2015596. Fax: 662-3547174. E-mail: scpcy@mucc.mahidol.ac.th (P.C.); Department of Biological Chemistry, University of Michigan, Ann Arbor, MI 48109-0606. Telephone: 734-764-9582. Fax: 734-764-3509. E-mail: dballou@umich.edu (D.P.B.).

‡ Mahidol University.

§ Chulalongkorn University.

|| University of Michigan.

⊥ University of New England.

10.1021/bi7006614 CCC: $37.00
Published on Web 06/27/2007

nas aeruginosa (*27*), *Escherichia coli* W (*4*, *28*), and *A. baumannii* (*3*, *29*−*31*). Interestingly, although catalyzing the same reaction, the enzymes fall into two distinct types: the reductases from *E. coli* and *P. aeruginosa* are dimers of 18−22 kDa monomers, while those from *A. baumannii* and *P. putida* are dimers of 34−36 kDa monomers (*1*, *3*−*5*). The reductase component (C_1) of HPAH from *A. baumannii* is isolated with one flavin mononucleotide (FMN) bound per subunit; its function is to provide the reduced FMN ($FMNH^-$) required for C_2 to hydroxylate HPA (*3*, *29*). Our previous studies showed that the binding of HPA allosterically stimulates the reduction of the C_1-bound FMN by reduced nicotinamide adenine dinucleotide (NADH) (*30*). This property has not been observed in the HPAH reductases from either *E. coli* (*4*) or *P. aeruginosa* (*27*). The oxygenases from *E. coli* and *P. aeruginosa* are dimers of 59 kDa monomers, while the oxygenase from *A. baumanii* is a tetramer of 47 kDa monomers. When amino acid sequences of the reductases and oxygenases are compared, it is clear that the two types of HPAH do not have a common origin (*29*). Although the different types of HPAH catalyze the same reaction, they have significant differences in the details of the mechanisms involved.

Thermodynamic data, including redox potentials and K_d values, imply that apoC_1 binds to $FMNH^-$ less tightly than to oxidized FMN and that the binding to $FMNH^-$ is even weaker in the presence of HPA (*30*). Our earlier investigations in which the rate constants for each step of catalysis were determined for the reactions of C_2 with $FMNH^-$, HPA, and O_2 [Figure 1 (*31*)] demonstrated preferential random-order interactions, with C_2 binding $FMNH^-$ first and then usually O_2, followed by HPA. C_2 was shown to bind tightly to $FMNH^-$ (K_d for C_2−$FMNH^-$ $\sim$ 1.2 μM), contrasting with its much weaker binding to oxidized FMN ($K_d = 250 \pm 50$ μM) (*31*). The rate of the reaction to form the C(4a)-hydroperoxy-FMN (the hydroxylating intermediate) when C_2 is 20 μM, $FMNH^-$ is 10 μM, and O_2 is 120 μM is 185 s^{-1} either when a mixture of C_2 and $FMNH^-$ is mixed with a solution containing O_2 or when a solution containing C_2 and O_2 is mixed with one containing $FMNH^-$. Therefore, the formation of the C_2−$FMNH^-$ complex is very rapid, much greater than the 185 s^{-1} rate to form the C(4a)-hydroperoxy-FMN (*31*) (Figure 1). This suggests that it is possible that C_1-bound FMN, after being reduced by NADH, could be released from C_1 and transferred to the active site of C_2 via diffusion without requiring specific protein−protein interactions between the two components.

Flavin transfer between components in this enzyme class has been investigated in several systems, and the answers obtained are diverse, e.g., simple flavin diffusion for *E. coli* HPAH (*4*, *28*), complex formation for bacterial luciferase (*32*,*33*) and alkane sulfonate monooxygenase (*34*, *35*), and a combination of diffusion and complex formation for styrene monooxygenase (*12*). However, no quantitative information as to how simple diffusion can be effective in these systems has been presented. Here, we report results from kinetics studies of the reactions involving C_1 and C_2 under steady-state and single-turnover conditions and compare these results to the known kinetics of the individual components (*30*, *31*). Our results clearly indicate that $FMNH^-$ can be delivered to the active site of C_2 equally well, whether from C_1 or directly from solution. The kinetics of transfer of $FMNH^-$ from C_1 to C_2 by diffusion can quantitatively account for catalysis. Thus, it is not necessary to form any complex between C_1 and C_2 during the catalytic hydroxylation reaction. Although complexes may form under some conditions, no tight complexes were detected in this work. In addition, we have shown that the C_1−C_2 system can function efficiently without added FMN, implying that the flavin can shuttle back and forth between the two proteins during catalysis.

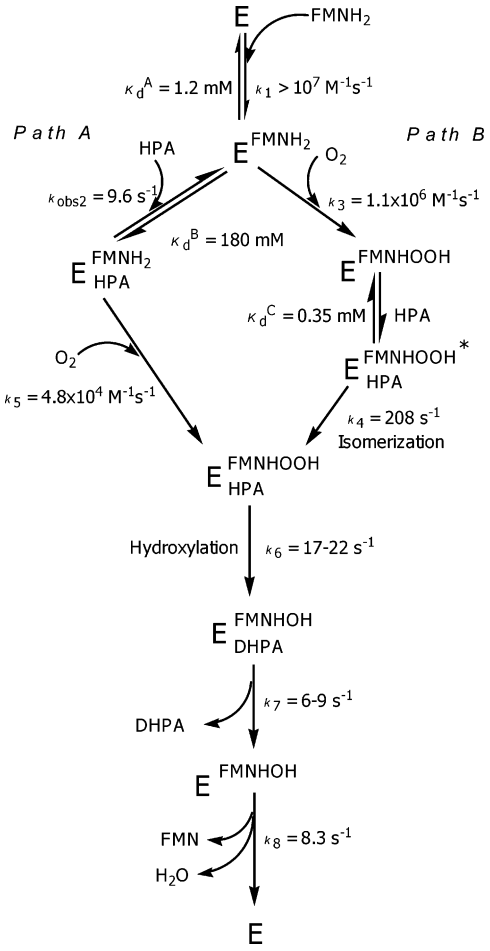

FIGURE 1: Kinetic mechanism of the oxygenase component (C_2) of HPAH from *A. baumanii* (*31*).

MATERIALS AND METHODS

Reagents. NADH, flavin adenine dinucleotide (FAD), glucose, and glucose oxidase were from Sigma. FMN was obtained by conversion of FAD to FMN by snake venom from *Crotalus adamanteus* (*36*). Concentrations of the following compounds were determined using known extinction coefficients at pH 7.0: NADH, $\epsilon_{340} = 6.22 \times 10^3$ M^{-1} cm^{-1}; FAD, $\epsilon_{450} = 11.3 \times 10^3$ M^{-1} cm^{-1}, FMN, $\epsilon_{446} = 12.2 \times 10^3$ M^{-1} cm^{-1}, HPA, $\epsilon_{277} = 1.55 \times 10^3$ M^{-1} cm^{-1} (*3*); Cytochrome *c* (cyt *c*) (reduced−oxidized forms), $\Delta\epsilon_{550} = 21 \times 10^3$ M^{-1} cm^{-1} (*37*). C_1 and C_2 used in this study were

[1] Abbreviations: HPA, *p*-hydroxyphenylacetate; HPAH, *p*-hydroxyphenylacetate hydroxylase; DHPA, 3,4-dihydroxy-phenylacetate; $FMNH^-$, reduced flavin mononucleotide; C_1, reductase component of HPAH from *A. baumannii*; C_2, oxygenase component of HPAH from *A. baumannii*; C_2−FMN, complex of C_2 and oxidized FMN; C_2−$FMNH^-$, complex of C_2 and reduced FMN; C_2−$FMNH^-$HPA, complex of C_2−$FMNH^-$ and HPA; cyt *c*, cytochrome *c*.

cloned, expressed, and prepared as previously described (*3*, *29*). The concentration of C_1 was estimated from the extinction coefficient, $\epsilon_{458} = 12.8 \times 10^3\ M^{-1}\ cm^{-1}$, and the concentration of C_2 was from the value (on the basis of the amino acid sequence) $\epsilon_{280} = 5.67 \times 10^4\ M^{-1}\ cm^{-1}$ (*30*, *31*).

Spectroscopic Studies. UV−vis absorbance spectra were recorded with a Hewlett-Packard diode array spectrophotometer (HP 8453A) or a Shimadzu 2501PC spectrophotometer. Fluorescence measurements were carried out with a Shimadzu RF5301PC spectrofluorometer. All spectral instruments were equipped with thermostated cell compartments.

Rapid Reaction Experiments. All reactions were carried out in buffer A: 50 mM sodium phosphate buffer at pH 7.0 and 4 °C, unless otherwise specified. When appropriate, solutions were made anaerobic by equilibrating with oxygen-free argon as described earlier (*31*). Rapid kinetics measurements were performed with Hi-Tech Scientific stopped-flow spectrophotometers, model SF-61DX in double-mixing mode or model SF-61SX in single-mixing mode. Optical path lengths of the observation cells were 1 cm. The stopped-flow instrument was made anaerobic by flushing the flow system with an anaerobic solution consisting of 400 μM glucose, 1 mg/mL glucose oxidase (15.5 unit/mL), and 4.8 μg/mL catalase in 50 mM sodium phosphate buffer at pH 7.0. An anaerobic glucose/glucose oxidase solution was allowed to stand in the flow system overnight, and the flow unit was then thoroughly rinsed with anaerobic buffer prior to experiments.

Apparent rate constants from kinetic traces were calculated from exponential fits using KinetAsyst 3 software (Hi-Tech Scientific, Salisbury, U.K.) or program A (written at the University of Michigan by Rong Chang, Jung-yen Chiu, Joel Dinverno, and David P. Ballou). FMN (alone or in complex with either C_1 or C_2) was reduced anaerobically in a tonometer with dithionite (~5 mg/mL stock solution in 100 mM potassium phosphate buffer at pH 7.0) delivered anaerobically from a syringe prior to reactions with O_2 in the stopped-flow apparatus. Reduction reactions were monitored spectrophotometrically. Buffer solutions containing various concentrations of oxygen were prepared by bubbling solutions with mixtures of certified nitrogen and oxygen.

Gel-Filtration Chromatography To Assess Affinities of C_1 to FMN and FMNH$^-$. The affinity of the C_1 active site for FMN was investigated by passing solutions of 32 μM oxidized C_1 in the presence of 200 μM HPA through a Sephadex G-25 gel-filtration column (1.4 × 11 cm) previously equilibrated with 50 mM sodium phosphate buffer at pH 7.0, 1 mM dithiothreitol (DTT), and 0.5 mM EDTA at 25 °C. This procedure was used to separate free FMN from enzyme-bound forms. In other experiments, 32 μM reduced C_1, either with or without 200 μM HPA was similarly passed through the same Sephadex G-25 gel-filtration column. NADH (1 mM) was included in the equilibration and elution buffers to maintain the FMN in the reduced state. The flow rate for elution was 1.5 mL/min. Fractions of 1.5 mL were collected from the column and left at room temperature for about 30 min until the reduced flavin (colorless upon elution) became fully oxidized (yellow) before analysis. Each of the fractions was monitored for protein and FMN concentrations by measuring the absorbance at 280 and 450 nm, respectively.

Table 1: Initial Rates of Product (DHPA) Formation Measured in Steady-State Kinetics[a]

added [FMN] (μM)	initial rate[b] (μM s^{-1}) (2 μM C_1 and 4 μM C_2)	initial rate[b] (μM s^{-1}) (4 μM C_1 and 4 μM C_2)	initial rate[b] (μM s^{-1}) (2 μM C_1 and 2 μM C_2)
0.0	3.9	3.7	3.5
1.0	3.8	3.7	
2.0	3.7	3.6	
4.0	3.7	3.5	
8.0	3.4	3.4	
16.0	3.2	3.1	

[a] Reactions were carried out by mixing a solution containing C_1 and C_2 (as indicated) and 100 μM HPA with buffers containing 80 μM NADH with or without free FMN in 50 mM sodium phosphate buffer at pH 7.0 and 25 °C in a stopped-flow spectrophotometer. Dihydroxyphenylacetate oxygenase was also included in the assays to convert DHPA into the yellow 5-carboxymethyl-2-hydroxymuconate semialdehyde that can be monitored at 420 nm (*3*). A calibration curve using authentic DHPA was used to correlate the absorbance at 420 nm to the concentration of DHPA formed. [b] Values are from three replica, and errors are less than 5%.

RESULTS

Steady-Steady Kinetics in the Presence of C_1 and C_2. Most steady-state kinetics studies of the two-component flavin-dependent hydroxylases have been carried out with flavin in great excess over the two enzymes. If the reductase used was to have a high catalytic turnover rate compared to the oxygenase (which is usually the case), the excess free reduced flavin produced could react with O_2 and lead to considerable H_2O_2 (and even superoxide). This would result in the overall hydroxylation being poorly coupled to the use of NADH. We have carried out experiments here to test whether excess FMN is necessary or whether the FMN that is bound to the reductase (C_1) as isolated is sufficient for efficient catalysis. Steady-state survey kinetics using 2 μM C_1, 4 μM C_2, 200 μM NADH, 120 μM HPA, and various concentrations of free FMN were monitored by measuring the NADH consumption at 340 nm in the stopped-flow instrument. It was observed that when the added FMN concentration was decreased from 1 to 0.01 μM, the initial rate only changed from 21.7 to 8.8 μM/s, less than 3-fold (data not shown). We also carried out reactions containing 100 μM HPA, 80 μM NADH, and various concentrations of free FMN (1, 2, 4, 8, and 16 μM) to test whether product formation was stimulated by added FMN. The initial rate of formation of DHPA was measured using 3,4-dihydroxyphenylacetate dioxygenase to convert the product to the highly colored 5-carboxymethyl-2-hydroxymuconate semialdehyde, which is easily detected (see Table 1) (*3*). The addition of free FMN did not increase the initial rate of product formation. In fact, the apparent rate seemed to be slightly smaller at high concentrations of free FMN (Table 1). It might be noted that at these higher FMN concentrations this apparent loss of activity could be due to the reduction of added FMN by the reductase, which would result in decreases of absorbance at 420 nm that could partially counter the increase as a result of the formation of the product. Thus, at this range of concentrations of C_1 and C_2, external FMN is not needed for catalysis. The flavin initially bound by C_1 can function as both a cofactor and substrate for C_2; FMN is reduced on C_1, transferred to C_2, where it reacts with O_2

and HPA to effect the hydroxylation, and then returns to C_1 to begin another catalytic cycle.

A steady-state kinetics study with no added FMN was therefore carried out in buffer A using the stopped-flow spectrophotometer. Assays contained 2 μM C_1, 4 μM C_2, and various concentrations of HPA (10, 20, 40, 80, 100, 120, 140, and 160 μM). Because the reaction of C_2-FMNH^- with O_2 is very fast, the concentration of O_2 was kept at 240 μM (aerobic), which is likely to be well in excess of K_m for O_2. The solutions containing the enzymes and various concentrations of HPA were mixed with 100 μM NADH, and the reactions were monitored at 340 nm. All concentrations are given as after mixing. It was found that HPA concentrations greater than 120 μM resulted in substrate inhibition, as described previously (*31*) and discussed below. Therefore, subsequent assays used HPA at 100 μM and various concentrations of NADH (10, 20, 40, 80, 100, 120, and 140 μM). Inhibition occurred at NADH concentrations $\geq$ 100 μM. The apparent V_{max} was determined to be 4 μM/s under these conditions, yielding an apparent $k_{cat} \sim 2\ s^{-1}$ (data not shown). This value is similar to the apparent rate constant of 1.8 s^{-1} calculated from single-turnover experiments for the last phase of the reaction of C_2-FMNH^- with these concentrations of HPA and O_2. In this last step, the C(4a)-hydroxy-FMN product formed from the hydroxylation reaction (via k_6 in Figure 1) loses H_2O (k_8 in Figure 1) to form oxidized FMN (*31*). As described below, high concentrations of HPA trap the C(4a)-hydroxy-FMN to retard its dehydration to form FMN. Thus, the dehydration of C_2 is the rate-limiting step of the overall hydroxylation reaction.

The coupling of product formation to NADH utilization was tested under the same conditions as used above for the steady-state kinetics study. The DHPA product was quantified by high-performance liquid chromatography (HPLC) analysis using NADH as the limiting substrate, and HPA was 120 μM. These experiments showed that an average of 86% of the NADH was used in the hydroxylation of HPA (data not shown). This value is similar to that determined from single-turnover reactions (~80%) when based on the amount of reduced flavin used in the reactions (*31*).

Overall, the results from the steady-state kinetics studies allow us to conclude that (a) no extra FMN (above that in the reductase) is required for effective catalysis, (b) the rates of product formation are nearly optimal under these conditions, and (c) $FMNH^-$ is transferred from the reductase to the oxygenase, with very little being oxidized while free in solution (i.e., there is good coupling).

Separation of FMN(H^-) from C_1 under Equilibrium Conditions. Experiments were carried out to examine qualitatively whether $FMNH^-$ binds less tightly to C_1 than does FMN and whether HPA has further effects on this putative differential binding. G-25 Sephadex gel-filtration chromatography (Figure 2) was used to separate free from bound FMN in both oxidized and reduced forms, as described in the Materials and Methods. The peak centered at fraction 6 contains all of the protein and therefore indicates the amount of flavin that is bound to C_1. Fractions 9−20 contain free flavin. When oxidized C_1 (no HPA present) was chromatographed, essentially all of the FMN eluted with the protein (data not shown), which is consistent with the known tight binding of FMN to C_1 (K_d = 6 nM at 4 °C) (*30*). The solid line of Figure 2 represents a chromatogram of oxidized C_1

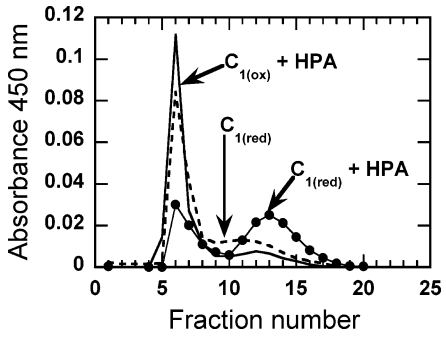

FIGURE 2: Gel-filtration chromatogram of $C_1-FMN(H^-)$ complexes in the absence and presence of HPA. Procedures are as described in the Materials and Methods. Under reducing conditions, the initial applied mixture and the fractions immediately eluting from the column were colorless, indicating that all of the flavin was reduced throughout the experiment. All of the protein eluted in fractions 5−8. Therefore, the peak absorbing at 450 nm in fraction 6 indicates the flavin bound to C_1, while the fractions including 9−20 indicate free flavin. Chromatograms are shown in the solid line for oxidized C_1 plus 200 μM HPA, a dotted line for HPA-free reduced C_1, and a line with filled circles for reduced C_1 plus 200 μM HPA.

in the presence of 200 μM HPA. Most of the FMN eluted with C_1 (holoenzyme), but a small amount of free FMN was detected, consistent with its slightly weaker binding in the presence of HPA [K_d = 38 nM at 4 °C (*30*)]. The dashed line is a chromatogram of reduced C_1 in the absence of HPA, while the line with filled circles represents a chromatogram of reduced C_1 in the presence of HPA (200 μM). The reduced state of C_1 was maintained by including 1 mM NADH in all buffers. Under reducing conditions, it is clear that a larger fraction of the flavin separated from the protein than under oxidizing conditions, and the presence of HPA resulted in most of the $FMNH^-$ eluting separately from C_1. This suggests that HPA significantly weakens the binding of $FMNH^-$ to C_1. In sections below, it will be shown that the binding of HPA to C_1 is a key factor controlling the transfer of $FMNH^-$ between the two protein components.

Attempt To Detect a Complex between C_1 and C_2. Experiments similar to those in Figure 2 but including C_2 (32 μM) and using G-100 Sephadex gel filtration were carried out to detect any C_1/C_2 complex that was present under various conditions. Any complex should be readily detected by this method because C_1 is a dimer of ~35 kDa monomers and C_2 is a tetramer of ~47 kDa monomers. Using oxidizing or reducing conditions, either in the presence or absence of HPA, no fractions that contained both C_1 and C_2 were found (data not shown); therefore, no stable complex was present.

Evidence that C_2 Binds $FMNH^-$ More Tightly than C_1. Efficient transfer of flavin between the two components during catalysis requires that $FMNH^-$ binds more tightly to C_2 (the hydroxylase) than to C_1 (the reductase) and that FMN binds more tightly to C_1. A solution containing 16 μM C_1 in buffer A was placed in a cuvette and made anaerobic. C_1 was reduced with a slight excess of sodium dithionite to ensure that the flavin remained reduced during the experiment; reduction of C_1 was monitored spectrophotometrically. When C_2 was tipped in from a side arm to be at a final concentration of 25 μM, the reduced flavin spectrum became perturbed as shown in Figure 3A. This perturbed spectrum is very similar to that when C_2 was added to a solution of free $FMNH^-$ (Figure 3B), strongly suggesting that it is due

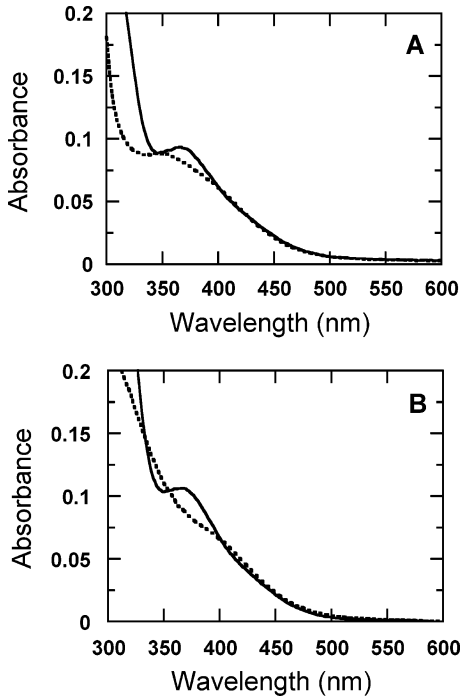

FIGURE 3: Evidence for binding $FMNH^-$ from C_1 or free in solution to the C_2 active site. (A) C_1 (16 μM) was reduced by a slight excess of sodium dithionite in an anaerobic cuvette, and its spectrum is shown as the dotted line. Then, C_2 (25 μM final) was added from the side arm into the cuvette, and the spectrum (—) was recorded. (B) This experiment was carried out in the same manner as in A, but 16 μM of free $FMNH^-$ was used instead of reduced C_1.

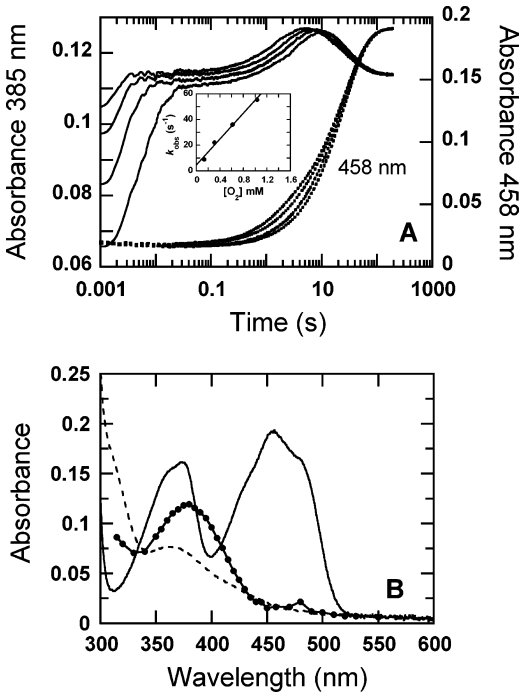

FIGURE 4: Reaction of reduced C_1 plus C_2 with oxygen. (A) Anaerobic solution of 15 μM reduced C_1 and 25 μM C_2 was mixed in a stopped-flow spectrophotometer with buffer A containing various concentrations of oxygen. The solid and dotted lines are traces measured at 385 and 458 nm, respectively, using oxygen concentrations of 0.13, 0.31, 0.61, and 1.03 mM (right to left). The inset shows the observed rate constants for the formation of C(4a)-hydroperoxy-FMN as a function of the oxygen concentration (the phase from 0 to 10 ms), from which a second-order rate constant of $1.2 \pm 0.1 \times 10^6$ M^{-1} s^{-1} was calculated. (B) Data from similar experiments as in A using 1.03 mM O_2 were recorded at selected wavelengths between 310 and 550 nm. A spectrum of the C(4a)-hydroperoxy-FMN intermediate (line with filled circles) was obtained by plotting the values from the traces at 10 ms. The spectrum has an absorption peak at 380 nm. The spectrum of reduced C_1 plus C_2 is shown as the dashed line, while that of the final oxidized species with FMN bound to C_1 is shown as the solid line.

to the binding of $FMNH^-$ to C_2. This conclusion implies that C_2 binds $FMNH^-$ with a $K_d \leq$ that for C_1. Note that the solid lines in parts A and B of Figure 3 are not exactly the same because only ~80% of $FMNH^-$ was transferred from C_1 to C_2 under the conditions used in Figure 3A (see explanation in the next experiment).

Reaction of Reduced C_1 Plus C_2 with Oxygen. If, in an anaerobic mixture of C_1 and C_2, most of the $FMNH^-$ is bound to C_2, such a mixture would be expected to react with O_2 essentially the same as when C_1 is not present. Buffer A containing 15 μM C_1 and 25 μM C_2 was stoichiometrically reduced with sodium dithionite (see the Materials and Methods) and then mixed at 4 °C in a stopped-flow spectrophotometer with buffer A containing various concentrations of oxygen (Figure 4). Concentrations are given in the caption as after mixing in the stopped-flow instrument. Reactions were monitored at 385 and 458 nm (Figure 4A). Kinetic analysis indicated that the reaction consisted of three phases, with the first phase being complete by ~ 0.02 s, the second phase being complete by ~5 s, and the third phase being complete by ~200 s. The first phase is shown by an increase of absorbance at 385 nm with no change at 458 nm, indicating the formation of C(4a)-hydroperoxy-FMN with no formation of oxidized FMN. A plot of k_{obs} for this phase was linearly dependent upon the oxygen concentration, with a second-order rate constant of $1.2 \pm 0.1 \times 10^6$ M^{-1} s^{-1} (inset of Figure 4A). These results are nearly identical to those for the formation of C(4a)-hydroperoxy-FMN in the reaction of a complex of C_2 and $FMNH^-$ (C_2—$FMNH^-$) with oxygen in the absence of C_1 [Table 2 (*31*)]. This finding is consistent with the binding experiment above, suggesting that a large fraction of the $FMNH^-$ had already been transferred from C_1 to C_2 before the reaction with O_2.

The second phase (0.2—9 s) is indicated by a slight increase in absorbance at both 385 and 458 nm and was also dependent upon the oxygen concentration, with an apparent bimolecular rate constant of ~340 M^{-1} s^{-1}. This rate constant corresponds to the rate of oxidation of reduced C_1 to generate H_2O_2 (320 M^{-1} s^{-1}) (*30*), indicating that the second phase was likely due to the oxidation of a small quantity of C_1—$FMNH^-$ remaining from the incomplete transfer of $FMNH^-$ to C_2. The amplitude of this phase at 458 nm suggests that about 20% of the $FMNH^-$ was bound to C_1. Given that the K_d for binding $FMNH^-$ to C_2 is 1.2 μM (*31*), this suggests that the K_d for $FMNH^-$ binding to C_1 is likely to be ≥ 5 μM. The third phase, shown by a decrease in absorbance at 385 nm and an increase at 458 nm at 0.37 ± 0.02 s^{-1}, was independent of the oxygen concentration and corresponded to the rate constant (0.35 s^{-1}) observed during the elimination of H_2O_2 from hydroperoxy-FMN in the reaction of C_2—$FMNH^-$ with oxygen in the absence of C_1 (*31*). Therefore, the reaction of C_2 plus reduced C_1 with O_2 is kinetically nearly equivalent to the reaction of O_2 with C_2—$FMNH^-$

Table 2: Kinetic and Thermodynamic Constants for the Reactions of Reduced C_1 Plus C_2 with O_2 and Reactions of C_2−FMNH$^-$ Alone (*31*)[a]

kinetic or thermodynamic constants	reduced C_1 plus C_2	C_2−FMNH$^-$
k_3, formation of C(4a)-hydroperoxy-FMN[b]	$1.2 \pm 0.1 \times 10^6$ M^{-1} s^{-1}	$1.1 \pm 0.1 \times 10^6$ M^{-1} s^{-1}
k_5, formation of C(4a)-hydroperoxy-FMN in the presence of HPA[b]	$5.0 \pm 0.3 \times 10^4$ M^{-1} s^{-1}	$4.8 \pm 0.2 \times 10^4$ M^{-1} s^{-1}
K_d^B, for the reduced enzyme/HPA complex[c]	123 ± 1 μM	180 ± 3 μM
K_d^C, for the enzyme-C(4a)-hydroperoxy-FMN/HPA complex[c]	0.41 ± 0.03 mM	0.35 ± 0.03 mM
k_4, for the isomerization of the C_2−C(4a)-hydroperoxy-FMN/HPA complex[c]	209 ± 4 s^{-1}	208 ± 4 s^{-1}
k_6, hydroxylation[b,c]	∼17−22 s^{-1}	∼17−22 s^{-1}
k_7, product releasing[b,c]	∼6−9 s^{-1}	∼6−9 s^{-1}
k_8, dehydration (and release of FMN)[d]	8.3 s^{-1}	8.3 s^{-1}

[a] Kinetic constants correspond to the labels in Figure 1. [b] Values from single-mixing stopped-flow experiments. [c] Values from double-mixing stopped-flow experiments. [d] Strongly dependent upon the HPA concentration.

alone, because most of the FMNH$^-$ initially bound to C_1 had been transferred to C_2 before the reaction with O_2.

Kinetic traces of the reaction described in Figure 4A using 1.03 mM oxygen were monitored at 5−10 nm intervals in the region of 315−550 nm. Values at the reaction time of 0.01 s were used to construct a spectrum of the C4a-hydroperoxy-FMN intermediate (Figure 4B). The spectrum (filled circles in Figure 4B) is typical for spectra of C(4a)-oxygenated flavin adducts (*38*−*41*) and the one observed during the reaction of C_2−FMNH$^-$ with oxygen (*31*). Note that because of the incomplete transfer of FMNH$^-$ from C_1 to C_2, by 10 ms under these conditions, the absorbance of the intermediate in Figure 4B is less than that from the reaction of C_2−FMNH$^-$ (*31*) or that shown in the next section (Figure 5). When the reaction was complete, the absorbance peaks at 375 and 458 nm because of FMN had resolved shoulders, characteristic of the C_1-bound FMN spectrum (solid line in Figure 4B) (*3*, *30*), consistent with it having been transferred back to C_1, where it can be re-reduced for subsequent catalytic reactions.

Reaction of Reduced C_1 Plus C_2 with Oxygen in the Presence of HPA. The results above suggested that the presence of HPA makes the transfer of FMNH$^-$ from C_1 to C_2 more favorable. To test this hypothesis, anaerobic buffer A containing 16 μM reduced C_1, 25 μM C_2, and 400 μM HPA was mixed in a stopped-flow spectrophotometer with buffer A containing 400 μM HPA and various concentrations of oxygen. The reaction monitored at 370 nm shows four phases (Figure 5A). At the highest oxygen concentration (the left most trace), the first phase was an increase of absorbance during the dead time until about 4 ms and the rate was dependent upon the oxygen concentration ($1.2 \pm 0.3 \times 10^6$ M^{-1} s^{-1}). This second-order rate constant is the same as that for the formation of C(4a)-hydroperoxy-FMN in the absence of HPA during the oxidation of C_2−FMNH$^-$ (*31*) and for the first phase of the reaction of the reduced C_1 plus C_2 with oxygen (Figure 4A). The second phase in Figure 5A consists of a large increase in absorbance from ∼4 ms to ∼0.1 s, and this rate was also dependent upon the oxygen concentration ($5.0 \pm 0.3 \times 10^4$ M^{-1} s^{-1}, inset of Figure 5A). This value is essentially the same as that previously measured for the reaction of oxygen with C_2−FMNH$^-$ in complex with HPA [Figure 1 and Table 2 (*31*)]. Therefore, the first and second phases are likely to be due to the formation of C_2−C(4a)-hydroperoxy-FMN intermediates in the HPA-free and HPA-bound forms. The third phase consists of a small decrease in absorbance between 0.1 and 1 s and was independent of the oxygen concentration, with an apparent rate constant of ∼17−22 s^{-1} (Figure 5A), similar to the hydroxylation step occurring in the reaction of oxygen with C_2−FMNH$^-$ in complex with HPA [Figure 1 and Table 2 (*31*)]. The fourth phase is seen as an absorbance decrease at 370 nm and a large increase at 458 nm (dotted-line traces), with an apparent rate constant of 1.1 s^{-1}. This phase was due to the dehydration of C(4a)-hydroxy-FMN to yield oxidized FMN and is dependent upon the concentration of HPA; when HPA is at 2 mM, an apparent rate constant of

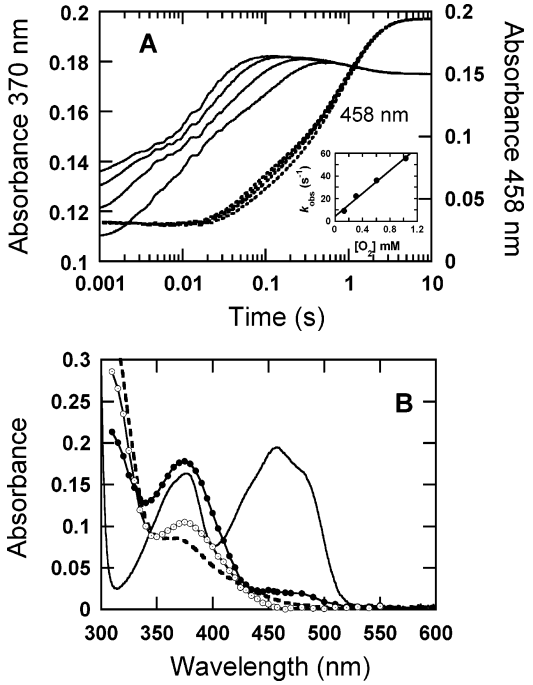

FIGURE 5: Reaction of reduced C_1 plus C_2 with oxygen in the presence of HPA. (A) Anaerobic solution of 16 μM reduced C_1, 25 μM C_2, and 400 μM HPA was mixed with buffer A containing 400 μM HPA and various concentrations of oxygen in a stopped-flow spectrophotometer. The solid and dotted lines are traces measured at 370 and 458 nm, respectively. Oxygen concentrations used were 0.13, 0.31, 0.61, and 1.03 mM oxygen (from right to left). All concentrations are indicated as after mixing. Apparent rate constants of the second phase are plotted versus the O_2 concentration in the inset to yield a second-order rate constant of $5.0 \pm 0.3 \times 10^4$ M^{-1} s^{-1}. The first phase (not plotted) yielded a rate constant of $1.2 \pm 0.1 \times 10^6$ M^{-1} s^{-1}. (B) Data from experiments similar to those in A using 1.03 mM O_2 were recorded at selected wavelengths between 310 and 550 nm. A spectrum of the C(4a)-hydroperoxy-FMN intermediate (line with filled circles) was calculated from the absorbance values at the reaction time of 80 ms and rate constants described in the text. The spectrum of reduced C_1 plus C_2 in the presence of 400 μM HPA is shown as a dashed line, while that of the final species is a solid line.

0.35 s^{-1} is observed. The presence of 2 mM HPA traps hydroxy-FMN, so that the loss of H_2O to form oxidized FMN occurs slowly (*31*).

Spectra of two intermediates were calculated from a set of traces similar to those shown in Figure 5A, recorded at 5−10 nm intervals from 315 to 550 nm. The first spectrum was plotted from the values observed at 4 ms. The second intermediate was calculated using absorbance values at the reaction time of 0.08 s, corrected for full formation using rate constants for the oxygen reaction of 54 s^{-1} (the O_2 reaction under these conditions in the presence of HPA), the hydroxylation step of 22 s^{-1}, and the dehydration step of 1.1 s^{-1}. The line with open circles represents a spectrum of C(4a)-hydroperoxy-FMN formed from that fraction (∼25%) of the enzyme that does not have HPA bound; it is similar in character to that shown in the previous section obtained without HPA (Figure 4B). The line with closed circles represents a spectrum of C(4a)-hydroperoxy-FMN formed by the end of the second phase, and it represents the spectrum of the HPA-bound form of the enzyme [which reacts more slowly with oxygen than the free enzyme (*31*)] plus that of any enzyme without HPA bound. It appears that the presence of HPA slightly shifts the spectrum to shorter wavelengths compared to that in Figure 4 (375 nm versus 380 nm). Overall, these results are very similar to those obtained without C_1 present (*31*) and are also consistent with most of the C_1-bound $FMNH^-$ having been transferred to C_2 in the presence of HPA before being mixed with O_2.

Determination of the Rate Constant for the Transfer of $FMNH^-$ from C_1 to C_2 in the Absence and Presence of HPA. From our earlier study (*31*), the rate constant for free $FMNH^-$ binding to C_2 (Figure 1) was estimated to be $>10^7$ M^{-1} s^{-1}. This large rate constant explains why mixing free $FMNH^-$ with an aerobic solution of C_2 resulted in the complete formation of C_2−C(4a)-hydroperoxy-FMN at the same rate as when preformed C_2−$FMNH^-$ was mixed with oxygen [the C(4a)-hydroperoxy-FMN intermediate forms with a second-order rate constant of 1.2×10^6 M^{-1} s^{-1} (*31*)]. Because the C(4a)-hydroperoxy-FMN forms very rapidly (see Figure 4A), its appearance can be used to indicate when $FMNH^-$ is transferred from C_1 to C_2. For example, if the transfer of $FMNH^-$ from C_1 to C_2 is much faster than the rate of the oxygen-dependent formation of C(4a)-hydroperoxy-FMN, the intermediate should form with the same second-order rate as when C_1 is absent (as in the reaction of the C_2−$FMNH^-$ complex). On the contrary, if the rate of $FMNH^-$ transfer is slower than the rate of the formation of C(4a)-hydroperoxy-FMN, the observed rate of its formation will indicate the rate of transfer and will not be second-order with respect to O_2. A solution of reduced C_1 was mixed in a stopped-flow spectrophotometer with solutions of C_2 in buffer A containing various concentrations of O_2. The reactions were monitored at 380 and 458 nm (Figure 6).

In the absence of HPA, C(4a)-hydroperoxy-FMN formed at only ∼0.35 s^{-1}, with some dependence on the O_2 concentration (380 nm, dotted lines), and this intermediate converted to oxidized FMN at 0.037 s^{-1} (458 nm, dotted line in Figure 6). Thus, in the absence of HPA, flavin transfer is slow and occurs at only ∼0.35 s^{-1}. Moreover, because it is so slow, some C_1−$FMNH^-$ becomes oxidized by its direct reaction with O_2 (note the 458 nm trace, dotted line, out to ∼10 s). In contrast to the reaction with C_1−$FMNH^-$, the

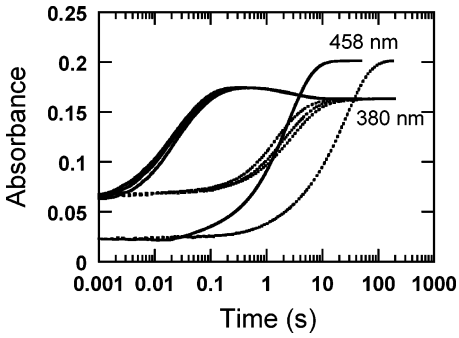

FIGURE 6: Transfer of the $FMNH^-$ from C_1 to C_2 in the absence and presence of HPA. Reactant concentrations are indicated as after mixing. Reduced C_1 (16 μM) was mixed with solutions of C_2 (25 μM) containing 0.13, 0.31, and 0.61 mM of O_2, and the reactions were monitored at 380 and 458 nm. Reactions in the absence of HPA are shown as dotted lines. Reactions in the presence of HPA are shown as solid lines.

reaction of free $FMNH^-$ with C_2 under these conditions has a rate of formation of the C(4a)-hydroperoxy-FMN of 185 s^{-1}; this intermediate converts to oxidized FMN very slowly at 0.037 s^{-1}, the same as observed in the above experiment (*31*).

The presence of 2 mM HPA dramatically changes these reactions. The solid lines in Figure 6 show the results of mixing reduced C_1 containing 2 mM HPA with solutions of C_2 also containing 2 mM HPA and various concentrations of O_2. At 380 nm, the observed rate constants for the formation of the C(4a)-hydroperoxy-FMN (first phase, 0.002−0.2 s) were all less than those for the reaction of C_2−$FMNH^-$ with O_2 (see Figure 4A and Table 2) and were not linearly dependent upon the oxygen concentration. The k_{obs} values for this phase ranged from 55 to 74 s^{-1} as O_2 varied from 0.13 to 1.03 mM. This indicates that the rate of transfer of $FMNH^-$ from C_1 to C_2 occurs at a rate that is ≥74 s^{-1}. The conversion of the C(4a)-FMN adduct to oxidized FMN under these conditions occurs at ∼0.35 s^{-1}, as shown by the trace recorded at 458 nm (solid line trace of 458 nm in Figure 6). In this reaction, hydroxylation proceeded at ∼20 s^{-1} to form C(4a)-hydroxy-FMN (k_6 in Figure 1), which has almost the same spectrum as C(4a)-peroxy-FMN. However, as discussed above, the presence of 2 mM HPA traps the hydroxy-FMN, so that the loss of H_2O to form oxidized FMN occurs at only 0.35 s^{-1}. Note that in the previous section this rate was 1.1 s^{-1} when less HPA (400 μM) was present (*31*). At very low concentrations of HPA, the rate of this process is extrapolated to be ∼8 s^{-1}, as indicated in Figure 1. It is a coincidence that, with this concentration of HPA (2 mM), the formation of FMN after hydroxylation (0.35 s^{-1}) is the same as the rate of transfer of $FMNH^-$ from C_1 to C_2 in the absence of HPA.

We also used a double-mixing stopped-flow approach to measure the rate constant for transfer of $FMNH^-$ from C_1 to C_2 in the absence of HPA. First, reduced C_1 (16 μM) was mixed with C_2 (25 μM) anaerobically and aged for various periods. Then, buffer that contained oxygen (0.5 mM after mixing) was added in the second mix, and the reactions were monitored at 380 nm to detect the rapid formation of C(4a)-hydroperoxy-FMN (Figure 7). At this concentration of O_2, the reaction with C_2−$FMNH^-$ completely forms C_2−C(4a)-hydroperoxy-FMN by 10 ms (*31*), so that its formation provides a good measure of the amount of $FMNH^-$ that has

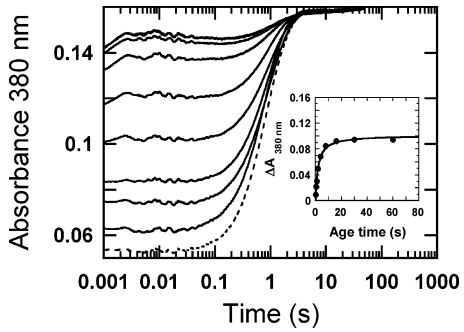

FIGURE 7: Determination of the rate of transfer of $FMNH^-$ from C_1 to C_2 in the absence of HPA. Reactant concentrations are indicated as after mixing. Reduced C_1 (16 μM) was mixed with C_2 (25 μM) anaerobically in the first mix of a double-mixing stopped-flow experiment. The reaction mixture was aged for 0.1, 0.5, 1, 2, 4, 8, 16, 30, and 60 s, before mixing with 0.5 mM oxygen. The formation of the $C_2-C(4a)$-hydroperoxy-FMN intermediate was indicated by the rapid increase of absorbance at 380 nm that occurred by 3 ms. The largest such rapid change occurred after the longest aging time. At short age times, very little increase at 380 nm occurs in the first 3 ms. The dotted line is a trace from an experiment in which reduced C_1 was mixed with O_2 in the absence of C_2. The inset shows differences in absorbance between each trace and the control experiment without C_2 at a reaction time of 0.01 s plotted against the age time. Plotting the absorbance change versus the aging time yielded a half-time ($t_{1/2}$) for the formation of the C_2-FMNH^- complex of 1.97 s, correlating with an observed rate constant for $FMNH^-$ transfer in the absence of HPA to be 0.35 s^{-1}.

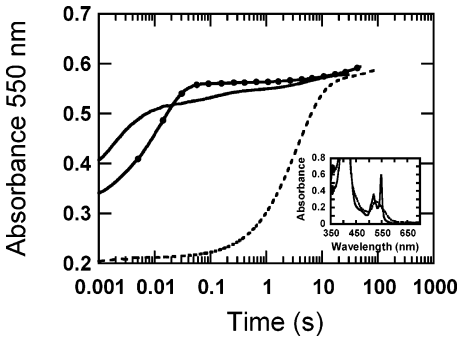

FIGURE 8: Reaction of cyt *c* with reduced C_1 in the presence and absence of HPA. All concentrations given are after mixing, and the experiments were carried out anaerobically using a stopped-flow spectrophotometer. The inset shows spectra of oxidized cyt *c* (•••) and reduced cyt *c* (—). The reduction of cyt *c* was monitored at 550 nm. Solid line (upper trace), $FMNH^-$ (8 μM) was mixed with oxidized cyt *c* (25 μM). Dashed line (lower trace), reduced C_1 (8 μM) was mixed with oxidized cyt *c* (25 μM). Line with filled circles (upper trace), reduced C_1 (8 μM) was mixed with oxidized cyt *c* (25 μM) in the presence of 2 mM HPA.

been transferred at any aging time after mixing. Figure 7 shows that with longer aging times there were larger absorbance increases by 10 ms, demonstrating that, when C_1-FMNH^- was incubated with C_2 for increasing periods of time, more $FMNH^-$ was transferred from C_1 to C_2, resulting in a greater formation of $C_2-C(4a)$-hydroperoxy-FMN in the rapid phase. A control experiment without C_2 present showed that no $C_2-C(4a)$-hydroperoxy-FMN was formed and the flavin simply reoxidized and then rebound to C_1 [dotted line of Figure 7 (*30*)]. A plot of the absorbance increases at 380 nm that had occurred at the reaction time of 10 ms versus the aging time (inset of Figure 7) represents the kinetics of transfer of $FMNH^-$ from C_1 to C_2 in the absence of HPA. A half time of 1.97 s was observed, corresponding to a rate constant of 0.35 s^{-1}, the same as obtained in the single mix experiment above. In the presence of HPA, the transfer is too fast ($\sim$80 s^{-1}) to resolve by our double-mixing technique.

Use of Cyt c To Measure the Release of $FMNH^-$ from C_1. Results presented in previous sections have shown that $FMNH^-$ bound to C_1 can be efficiently transferred to C_2 and react at the C_2 active site; there was no indication that C_1 and C_2 need to interact to facilitate this transfer (Figures 2−7). Moreover, the dissociation of $FMNH^-$ from C_1, which allows for its binding to C_2, was clearly shown to be facilitated by HPA binding to C_1 (Figure 6). In the following experiments, we used the reduction of cyt *c* by C_1-FMNH^- as a second approach to examine whether $FMNH^-$ is released from C_1 at the same rate as the transfer of $FMNH^-$ to C_2 described in the previous section. It is known that the reduction of cyt *c* by free $FMNH^-$ is very fast and occurs in one-electron steps (*37*, *42*−*44*). Reduction of cyt *c* by free $FMNH^-$ was carried out as a control experiment as described in Figure 8. Reduction of cyt *c* by $FMNH^-$ can be monitored by the increase of absorbance at 550 nm because of the appearance of the α band of reduced cyt *c* (inset of Figure 8). Although the reaction (solid line) exhibits complex kinetics, the reduction of cyt *c* by $FMNH^-$ was complete by 20 ms. About 50% of the change occurred in the dead time of the stopped-flow instrument, and the remainder occurred with an observed rate constant of approximately 500 s^{-1} (the second electron transfer). As expected, the change of absorbance up to 20 ms is equivalent to the reduction of 2 molecules of cyt *c*/molecule of $FMNH^-$ present. The slower phases are probably due to the presence of a small excess of dithionite initially in the $FMNH^-$ solution and possibly to some photochemistry. In the following experiments, it was assumed that cyt *c* would not react rapidly with $FMNH^-$ bound to C_1 (this was found to be true, see below), so that the kinetics of the reduction of cyt *c* by reduced C_1 in the absence and presence of HPA would indicate the rates of dissociation of $FMNH^-$ from the C_1 active site. Subsequently, the same reduction of cyt *c* was investigated in the presence of C_2. If a specific interaction between reduced C_1 and C_2 occurs during transfer, the kinetics of cyt *c* reduction by C_1 would be significantly affected by the presence of C_2.

When cyt *c* was mixed with reduced C_1 under the same conditions as in the control experiment (above), cyt *c* was reduced with an observed rate constant of only $\sim$0.35 s^{-1} (dashed line in Figure 8), the same rate constant as observed for the $FMNH^-$ transfer in the absence of HPA (Figures 6 and 7). This suggests that, in the absence of HPA, the release of $FMNH^-$ from C_1 occurs at 0.35 s^{-1} and is rate-limiting in the transfer of $FMNH^-$ from C_1 to C_2. This result also implies that the C_1-bound $FMNH^-$ does not react rapidly with cyt *c*; the rate of the reaction is likely to be much less than 0.35 s^{-1}.

When the same experiment was carried out again but in the presence of 2 mM HPA, a very rapid phase of reduction of cyt *c* occurred in the dead time, typical of that of free flavin (about 40% of the total change), implying that $\sim$40% of the $FMNH^-$ was not bound to C_1 when HPA was present. This step was followed by further reduction of cyt *c* with an observed rate constant of $\sim$80 s^{-1} (the filled-circle line in Figure 8 up to 40 ms). Thus, the bound flavin reacted with

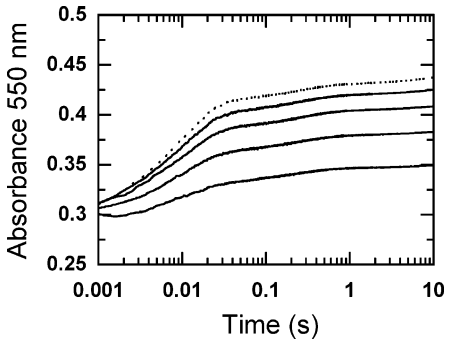

FIGURE 9: Reduction of cyt *c* by reduced C_1 in the presence of C_2. All concentrations given are after mixing, and solutions contained 2 mM HPA. Experiments were carried out using a stopped-flow spectrophotometer. The reduction of cyt *c* was monitored at 550 nm. Reduced C_1 (8 μM) was mixed with air-saturated buffers containing oxidized cyt *c* (25 μM) and various concentrations of C_2 (16, 40, 100, and 245 μM, upper to lower solid line traces). A control experiment in which the same concentration of reduced C_1 and HPA was mixed with cyt *c* without C_2 under the same conditions is shown as the dotted line.

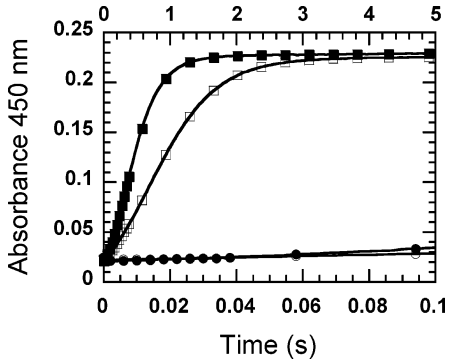

FIGURE 10: Reaction of $FMNH^-$ with O_2 with and without superoxide dismutase. A solution of $FMNH^-$ (20 μM) was mixed with aerobic buffer (130 μM) at 4 °C. Reactant concentrations are as after mixing. Traces with filled squares or circles do not have superoxide dismutase, while traces with open circles and squares have superoxide dismutase. The upper traces are 0−5 s, and the lower traces are 0−0.1 s, full scale.

cyt *c* at ~80 s^{-1}, which is similar to the rate of transfer of $FMNH^-$ from C_1 to C_2 as discussed above. Note that, in the presence of HPA, a larger portion of $FMNH^-$ was free than when HPA was absent, which is consistent with HPA decreasing the affinity between C_1 and $FMNH^-$ as indicated in the gel-filtration experiments (Figure 2). Thus, we conclude that the release of $FMNH^-$ from C_1 is the process that governs the rate of flavin transfer from C_1 to C_2 and HPA stimulates this rate by ~200-fold; diffusion and binding to C_2 are very fast.

In the next experiment, we examined whether specific interactions between C_1 and C_2 are required for the dissociation of $FMNH^-$ from C_1. If the efficient transfer of $FMNH^-$ from C_1 to C_2 in the presence of HPA requires specific interactions between the two proteins, C_2 would be expected to exclude or alter the kinetics of cyt *c* reduction by reduced C_1. A solution containing reduced C_1 and 2 mM HPA was mixed with an air-saturated solution of cyt *c* and various concentrations of C_2, and the reduction of cyt *c* by the $FMNH^-$ from C_1 was monitored at 550 nm (Figure 9). Because free $FMNH^-$ binds very rapidly to C_2, there was no need in this experiment to carry out the reaction anaerobically. The reaction traces in Figure 9 show that the rate constants observed (~80 s^{-1}) for the reduction of cyt *c* by $FMNH^-$ from C_1 (reactions up to ~40 ms) were independent of the concentration of C_2 and the same as that previously determined for the dissociation of $FMNH^-$ from C_1 in the absence of C_2 (Figure 8). This is because the reduction of cyt *c* is limited by the dissociation process, and C_2 has no influence on the dissociation of $FMNH^-$ from C_1. However, the amplitude of the absorbance change decreased with increasing concentrations of C_2, indicating that C_2 competed with cyt *c* for $FMNH^-$ that had been released from C_1 at ~80 s^{-1}. It should be emphasized that, even with the concentration of C_2 much greater than that of cyt *c* (up to ~10-fold or 245 μM), the same rate of reduction of cyt *c* was still observed (the lowest line, Figure 9), indicating that there is no specific protein interaction between C_1 and C_2 to facilitate this $FMNH^-$ transfer process.

Oxidation of Free $FMNH^-$ with and without Superoxide Dismutase. The traces shown in Figure 10 demonstrate that, when $FMNH^-$ reacts with O_2 at 10.5% saturation (half of the concentration of aerobic solutions or ~130 μM after mixing), very little $FMNH^-$ is oxidized in the first 0.1 s. Only 3 and 6% of the $FMNH^-$ was oxidized by 0.1 s with and without superoxide dismutase present, respectively. This experiment demonstrates that, in the presence of HPA, $FMNH^-$ can dissociate from C_1 with a rate of 80 s^{-1} and rapidly bind to C_2 with a rate of $\geq 10^7$ M^{-1} s^{-1} before its reaction with O_2 can occur.

DISCUSSION

Two main findings come from the work described here. First, it is demonstrated that the C_1/C_2 system can function efficiently with no added flavin; the flavin on C_1 as isolated is sufficient for nearly full activity of the system. Second, it has been demonstrated that the reduced flavin ($FMNH^-$) can be readily transferred from C_1 to C_2 via simple diffusion without requiring any protein−protein interactions. Moreover, the kinetic measurements reported here show quantitatively why simple diffusion can function successfully in catalysis.

Results from steady-state kinetics experiments (Table 1) have shown that, when C_1 and C_2 are in the micromolar range, exogenous flavin added has very little influence on the rate of product formation. The thermodynamics of binding for reduced and oxidized FMN to each of the components are appropriate for fostering the passing of FMN in a ping-pong fashion between the components of HPAH during catalysis. C_1 binds tightly to oxidized FMN with a K_d of 0.006 μM in the absence of HPA and a K_d of 0.038 μM in its presence (*30*). The gel-filtration experiments (Figure 2) showed that virtually all of the FMN eluted with C_1, which is consistent with the above K_d. In contrast, $FMNH^-$ binds to C_1 significantly less tightly than does FMN; a considerable fraction eluted separately from C_1 when HPA was not present, and about 50% eluted separately from C_1 in its presence. The K_d for the C_2−$FMNH^-$ complex is 1.2 μM, while that for the C_2−FMN complex is ~250 μM (*31*). These results demonstrate that in the presence of both proteins FMN binds more tightly to C_1 and $FMNH^-$ binds more tightly to C_2, as required for efficient catalysis.

After completion of the hydroxylation reaction on C_2, the resulting oxidized FMN dissociates from C_2 and rebinds to

C_1. Our stopped-flow results (discussed below) and the final spectrum showing characteristics of the C_1-bound flavin after completion of the single-turnover reaction of C_1 and C_2 (Figures 4B and 5B) demonstrate that FMN in its appropriate oxidation states can be readily transferred between C_1 and C_2; added free flavin is not needed in this system for efficient hydroxylation to occur (Figures 3−6). Given the K_d values of the functional complexes, C_2−$FMNH^-$ and C_1−FMN (1 and 0.038 μM, respectively), efficient passage of the flavin between the components is feasible if the concentration of C_2 is higher than 1 μM and the concentration C_1 is higher than 0.05 μM. Previously, Louis et al. have estimated the concentrations of the oxygenase and reductase components of HPAH in *E. coli* cells to be ∼122 and ∼15 μM, respectively (*28*). Thus, if C_1 and C_2 are present in quantities as low as one-tenth of those of the *E. coli* system, its K_d values for $FMN(H^-)$ would permit each component to efficiently sequester the oxidized or reduced FMN released from the other and extra FMN added would not significantly improve the efficiency of the system.

It should be noted that, in our earlier report on steady-state kinetic studies of C_1 and C_2, the rate of product formation was influenced by the concentration of free flavin (*3*). In retrospect, it is likely that this was due to the low concentrations of C_1 and C_2 (1−10 nM) used in the assays, causing the enzymes to exist mostly in the free form; adding extra flavin enhanced the formation of the C_2−$FMNH^-$ complex and therefore increased the rate of hydroxylation (*3*). It can be noted that most steady-state studies previously reported for two-component flavin-dependent hydroxylase systems used very small concentrations of enzymes, which, as noted above, are not likely to mimic those found in the bacteria.

In mixtures of reduced C_1 plus C_2, $FMNH^-$ is primarily bound to C_2, especially when HPA is present. This was shown by several experiments. First, when reduced C_1 and C_2 are added together at equilibrium, the spectrum of the $FMNH^-$ changes to that of the flavin bound to C_2 (Figure 3). Second, reactions in which O_2 is mixed with solutions containing reduced C_1 plus C_2 (in the absence or presence of HPA; Figures 4 and 5) are very nearly the same as corresponding reactions in which O_2 is mixed with solutions containing C_2 prebound to $FMNH^-$ or when solutions of C_2 and O_2 react with $FMNH^-$ (*31*). Table 2 compares kinetic and thermodynamic constants for the reactions of O_2 with C_2 in the presence and absence of reduced C_1. All parameters for the reaction of oxygen with reduced C_1 plus C_2 are very similar to those for C_2−$FMNH^-$ alone, consistent with the $FMNH^-$ being primarily on C_2. The overall conclusion is that, in mixtures of reduced C_1 and C_2, $FMNH^-$ initially bound to C_1 will be transferred to the C_2 active site.

The binding of free $FMNH^-$ to C_2 must be faster than the autoxidation of $FMNH^-$ if simple diffusion is to be effective in transferring $FMNH^-$ from C_1 to C_2; this would avoid wasteful auto-oxidation of the flavin during the transfer. Additionally, the regulation of the reduction and release of $FMNH^-$ from C_1 by HPA would also prevent the reductase from becoming a good oxidase. Our previous results have shown that $FMNH^-$ binds to C_2 very rapidly (we estimate these reactions to be ≥ 500 s^{-1} when C_2 is 25 μM) (*31*). When reduced C_1 was reacted with a mixture of C_2 and O_2 (no pre-equilibration), the reactions were highly dependent upon the presence of HPA (Figure 6). In the absence of HPA, the reaction of a mixture of C_2 and 130 μM O_2 with reduced C_1 to form the C(4a)-hydroperoxy-FMN intermediate on C_2 occurred with an observed rate of ∼0.35 s^{-1}. The double-mixing experiment shown in Figure 7 confirmed that, in the absence of HPA, $FMNH^-$ was transferred from C_1 to C_2 in a first-order reaction, with the same rate constant of only 0.35 s^{-1}.

In the presence of HPA, the reaction of reduced C_1 with a mixture of C_2 and oxygen formed C(4a)-hydroperoxy-FMN and reached a maximum rate of ∼80 s^{-1}. This rate was only partially dependent upon the O_2 concentration and was followed by hydroxylation reactions very similar to those observed with C_2 alone. At 130 μM O_2, the observed rate of formation of the C(4a)-hydroperoxy-FMN was 55 s^{-1}, which is just what would be expected for a consecutive reaction in which dissociation of $FMNH^-$ from C_1 at ∼80 s^{-1} was followed by a reaction of oxygen with C_2 in complex with $FMNH^-$ at ∼185 s^{-1}. The rates of reactions of C_1 with O_2 in the presence of HPA but in the absence of C_2 were ∼80 s^{-1} because, although $FMNH^-$ is released from C_1 at ∼80 s^{-1}, in contrast to the reactions involving C_2, reactions of O_2 with $FMNH^-$ are not very fast (see below). Under conditions that assays are usually carried out using very small concentrations of reductase, this slow oxidation of reduced flavin is sufficient to keep up with catalysis.

In this work, we have obtained several lines of evidence that rule out the necessity of C_1/C_2 complexes being involved in transferring reduced flavin from C_1 to C_2. No such complex can be isolated by gel filtration under oxidized or reduced conditions in either the presence or absence of HPA. The results from studies using cyt *c* show that the rates of transfer of flavin are independent of any transient complexes between C_1 to C_2. Cyt *c* was reduced by the complex of C_1 with $FMNH^-$ in the absence of HPA at an observed rate of 0.35 s^{-1}, the same rate as its transfer to C_2. In the presence of HPA, the rate was ∼80 s^{-1} (Figure 8), also in close agreement with the rates of transfer to C_2. Finally, we found that C_2 can compete with cyt *c* for $FMNH^-$ as it is released from C_1; the observed rate for the reduction of cyt *c*, even in the presence of C_2, was still ∼80 s^{-1}. This is not the sum of the two reactions with $FMNH^-$ because the rate constant for the release of $FMNH^-$ from C_1 (80 s^{-1}) is the rate-determining step of this process (Figure 9).

The recently determined X-ray structure of C_2 and its complexes with $FMNH^-$ and HPA offer an explanation of how C_2 can bind $FMNH^-$ so rapidly (*45*). The isoalloxazine of $FMNH^-$ binds to C_2 at the dimeric interface, and the overall structures of apoC_2 and C_2−$FMNH^-$ are very similar, implying that the C_2 structure can efficiently bind $FMNH^-$ without requiring any major structural changes or physical interactions with C_1.

It is not surprising that diffusion is a suitable mechanism for the transfer of $FMNH^-$ to the oxygenases of these two-component flavin-dependent hydroxylases. The reaction of free $FMNH^-$ with O_2 is autocatalytic, and although the overall reaction is relatively fast ($t_{1/2}$ ∼ 0.5 s, depending upon the O_2 concentration, temperature, etc.), the initial rate of oxidation is quite slow. The equations below illustrate the important reactions involved in the autocatalytic oxidation of $FMNH^-$ (*46*−*48*).

$$FMNH^- + O_2 \xrightarrow{\text{slow}} FMNH^\bullet + O_2^{\bullet-} \quad \text{(a)}$$

$$H^+ FMNH^\bullet + O_2^{\bullet-} \xrightarrow{\text{fast}} FMNHOOH \quad \text{(b)}$$

$$FMNHOOH \xrightarrow{\text{fast}} FMN + H_2O_2 \quad \text{(c)}$$

$$FMNH^\bullet + O_2 \xrightarrow{\text{very fast}} FMN + O_2^{\bullet-} \quad \text{(d)}$$

$$H^+ + FMNH^- + FMN \overset{\text{very fast}}{\rightleftharpoons} 2FMNH^\bullet \quad \text{(e)}$$

$$2H^+ + FMNH^- + O_2^{\bullet-} \xrightarrow{\text{fast?}} FMNH^\bullet + H_2O_2 \quad \text{(f)}$$

$$FMNH^\bullet + O_2^{\bullet-} \xrightarrow{\text{very fast}} FMN + H_2O_2 \quad \text{(g)}$$

$$2O_2^{\bullet-} + 2H^+ \xrightarrow{\text{very fast}} O_2 + H_2O_2 \quad \text{(h)}$$

Bruice and colleagues have estimated reaction a to be ~250 M^{-1} s^{-1} at 25 °C, which would give a rate of 0.025 s^{-1} at 100 μM O_2. On the other hand, reaction d is very fast. Furthermore, as oxidized FMN is produced, it reacts with $FMNH^-$ to form more $FMNH^\bullet$ that can react very fast (reaction e), leading to the observed autocatalysis. Additionally, superoxide, which is produced from reactions a and d, also reacts with various reduced forms of flavin (e.g., reactions f and g) to enhance the autocatalysis (*47*, *48*). Superoxide dismutase, which is present in most organisms, slows the reaction ~2-fold by eliminating reactions d and e while enhancing reaction h, as seen in Figure 10. Figure 10 demonstrates that any reasonably rapid binding process will permit the $FMNH^-$ to diffuse and bind to the partner oxygenase before it reacts with O_2. For example, a binding rate constant of 10^6 M^{-1} s^{-1} and a concentration of oxygenase of 10^{-5} M would give a rate of 10 s^{-1}, which would trap most of the reduced flavin before significant autoxidation occurred. With C_2, the binding rate constant is $\geq 10^7$ M^{-1} s^{-1}, giving an observed rate $\geq$ 100 s^{-1}. As mentioned above, the cellular concentrations of these oxygenase systems are likely to be at least 10 μM because they are induced to provide a major source of carbon to the bacteria (*28*).

Most evidence obtained on the mechanism of transfer of reduced flavin between reductases and oxygenases in other two-component systems is inconclusive. Reported kinetic parameters do not firmly establish if rapid diffusion or complex formation is the sole means for transfer of reduced flavin to the oxygenase in each system. A flavin-diffusion transfer model has been favored for *E. coli* HPAH because the oxygenase component binds to reduced FAD with a K_d of 70 nM, whereas it binds to oxidized FAD with a K_d of 6 μM (*28*). The *E. coli* HPAH was even able to catalyze the hydroxylation reaction, while both components were separated by a dialysis membrane (*4*), and it was also shown that the flavin reductases of other systems are able to replace the *E. coli* reductase and efficiently generate reduced FAD for its oxygenase (*28*). These rule out the necessity of specific interactions. However, the results presented here quantitatively show how this is possible and that diffusion is not only possible but also effective.

In the system involving biosynthesis of actinorhodin in *Streptomyces coelicolor*, an oxygenase component binds to $FMNH^-$ with a K_d of 0.39 μM and to FMN with a K_d in the range of 19−26 μM, while the reductase binds FMN more tightly than $FMNH^-$ (*20*). In styrene monooxygenase from *Pseudomonas* sp. VLB120, FAD binds to the oxygenase with a K_d of 21 μM and to the reductase with a K_d of 2.3 μM (*11*). These binding parameters are appropriate for the flavin transferring between the reductase and oxygenase proteins during catalysis, suggesting that the flavin in these other enzymes could also be transferred via rapid diffusion. In styrene monooxygenase from *Pseudomonas* sp., the oxygenase (SMOA) binds to reduced FAD 137-fold more tightly than to oxidized FAD [K_d for binding reduced FAD is 0.5 μM (*12*)]; however, the simulation of steady-state kinetics results suggested a model where both flavin diffusion and complex formation are involved (*12*). However, in contrast to our study here, in these other systems, kinetics showing how the oxygenase can bind reduced flavin very rapidly and thus avoid autoxidation have not yet been reported.

Direct channeling or complex formation has been proposed to be the mode of flavin transfer in several systems. Evidence for channeling has been presented by Tu et al. for bacterial luciferase and its reductase systems (*18*, *49*). Data from fluorescence anisotropy measurements of eosin-labeled reductase in the presence of luciferase have provided evidence for complexes (*32*), and fluorescence energy transfer between luciferase and yellow fluorescent protein (YFP) was observed in the coupled reaction of luciferase and the reductase fused with YFP (*33*). In alkane sulfonate monooxygenase, a model involving complex formation has been favored on the basis of altered steady-state kinetics of the reductase component when the oxygenase was included (*34*) and, recently, by detection of a complex by affinity chromatography and cross-linking experiments (*35*).

Our findings indicate the important role of HPA in regulating the rapid transfer of $FMNH^-$ between components in the HPAH system. Without HPA, the reduction of C_1-bound FMN by NADH is 14.7 s^{-1} (*30*) and the "off" rate of $FMNH^-$ from C_1 is 0.35 s^{-1} (Figures 6−8), rendering the overall production of free $FMNH^-$ to be rather slow (Figure 11A). In the presence of HPA (Figure 11B), the observed rate constant for the reduction of FMN is 300 s^{-1} (*30*), while the observed "off" rate constant is ~80 s^{-1} (Figures 6 and 8). Thus, it would appear that HPA, a substrate for the oxygenase component, allosterically influences the reactivity of the reductase and controls the overall rate of production of $FMNH^-$. In the absence of HPA, the hydroxylation system thereby avoids wasteful production of $FMNH^-$ to minimize the generation of H_2O_2 and consumption of the cellular reductant, NADH.

When the overall kinetic constants are considered, the rate-limiting step in the reaction of C_1 and C_2 is identified to be the step in which the C(4a)-hydroxy-FMN intermediate dehydrates to return back to the oxidized species (Figure 1). The rate of this step is 1.8 s^{-1} in the presence of 100 μM HPA, similar to the value of k_{cat} (~2 s^{-1}) obtained from the steady-state assays (see the Results). The rate of this step is even less when the concentration of HPA is increased, because the enzyme becomes trapped as the dead-end C(4a)-hydroxy-FMN/HPA complex (*31*). It is interesting that the transfer of $FMNH^-$ from C_1 to C_2 (74 s^{-1}; Figure 6) is not remotely rate-limiting in this reaction, although this step requires intermolecular flavin transfer. During steady-state

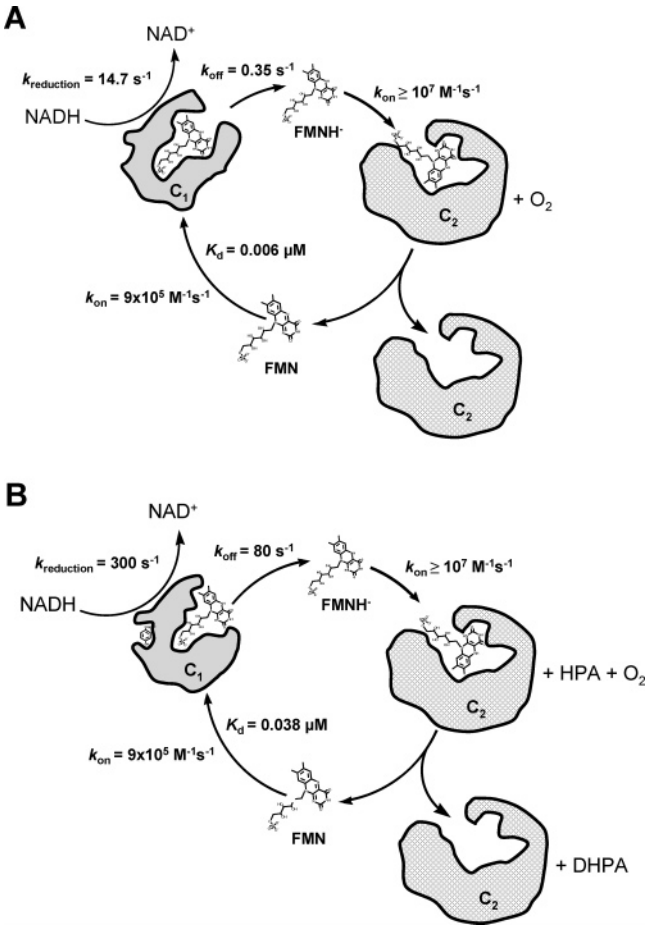

FIGURE 11: Flavin-diffusion transfer model. (A) In the absence of HPA, the reduction of the C_1-bound FMN by NADH occurs at the rate of 14.7 s^{-1}. The reduced FMN is then slowly released from C_1 (0.35 s^{-1}), and it diffuses to the C_2 active site. (B) In the presence of HPA, C_1 undergoes a conformational change that results in a large increase of the reduction rate (300 s^{-1}) and a more rapid dissociation rate of $FMNH^-$ from C_1 (80 s^{-1}) .

conditions in the presence of HPA, the flavin is trapped mostly on C_2 as the C(4a)-hydroxy-FMN/HPA complex.

In conclusion, our study has clearly illustrated that the unstable cofactor, $FMNH^-$, in the catalytic reactions of a two-component enzyme system, can be transferred between proteins efficiently, with no protein complexes being necessary. With HPAH from *A. baumanii*, HPA regulates the reduction and release of $FMNH^-$ from the reductase, enabling the transfer of $FMNH^-$ by rapid diffusion to the oxygenase.

REFERENCES

1. Ballou, D. P., Entsch, B., and Cole, L. J. (2005) Dynamics involved in catalysis by single-component and two-component flavin-dependent aromatic hydroxylases, *Biochem. Biophys. Res. Commun. 338*, 590−598.
2. van Berkel, W. J. H., Kamerbeek, N. M., and Fraaije, M. W. (2006) Flavoprotein monooxygenases, a diverse class of oxidative biocatalysts, *J. Biotechnol. 124*, 670−689.
3. Chaiyen, P., Suadee, C., and Wilairat, P. (2001) A novel two-protein component flavoprotein hydroxylase, *Eur. J. Biochem. 268*, 5550−5561.
4. Galan, B., Diaz, E., Prieto, M. A., and Garcia, J. L. (2000) Functional analysis of the small component of the 4-hydroxyphenylacetate 3-monooxygenase of *Escherichia coli* W: A prototype of a new Flavin:NAD(P)H reductase subfamily, *J. Bacteriol. 182*, 627−636.
5. Arunachalam, U., Massey, V., and Vaidyanathan, C. S. (1992) *p*-Hydroxyphenylacetate-3-hydroxylase. A two-protein component enzyme, *J. Biol. Chem. 267*, 25848−25855.
6. Kim, I. C., and Oriel, P. J. (1995) Characterization of the *Bacillus stearothermophilus* BR219 phenol hydroxylase gene, *Appl. Environ. Microbiol. 61*, 1252−1256.
7. Kirchner, U., Westphal, A. H., Muller, R., and van Berkel, W. J. H. (2003) Phenol hydroxylase from *Bacillus thermoglucosidasius* A7, a two-protein component monooxygenase with a dual role for FAD, *J. Biol. Chem. 278*, 47545−47553.
8. Gisi, M. R., and Xun, L. (2003) Characterization of chlorophenol 4-monooxygenase (TftD) and NADH:flavin adenine dinucleotide oxidoreductase (TftC) of *Burkholderia cepacia* AC1100, *J. Bacteriol. 185*, 2786−2792.
9. Louie, T. M., Webste, C. M., and Xun, L. (2002) Genetic and biochemical characterization of a 2,4,6-trichlorophenol degradation pathway in *Ralstonia eutropha* JMP134, *J. Bacteriol. 184*, 3492−3500.
10. Becker, D., Schrader, T., and Andreesen, J. R. (1997) Two-component flavin-dependent pyrrole-2-carboxylate monooxygenase from *Rhodococcus* sp., *Eur. J. Biochem. 249*, 739−747.
11. Otto, K., Hofstetter, K., Rothlisberger, M., Witholt, B., and Schmid, A. (2004) Biochemical characterization of StyAB from *Pseudomonas* sp. strain VLB120 as a two-component flavin-diffusible monooxygenase, *J. Bacteriol. 186*, 5292−5302.
12. Kantz, A., Chin, F., Nallamothu, N., Nguyen, T., and Gassner, G. T. (2005) Mechanism of flavin transfer and oxygen activation by the two-component flavoenzyme styrene monooxygenase, *Arch. Biochem. Biophys. 442*, 102−116.
13. Kadiyala, V., and Spain, J. C. (1998) A two-component monooxygenase catalyzes both the hydroxylation of *p*-nitrophenol and the oxidative release of nitrite from 4-nitrocatechol in *Bacillus sphaericus* JS905, *Appl. Environ. Microbiol. 64*, 2479−2484.
14. Uetz, T., Schneider, R., Snozzi, M., and Egli, A. (1992) Purification and characterization of a two-component monooxygenase that hydroxylates nitrilotriacetate from "Chelatobacter" strain ATCC 29600, *J. Bacteriol. 174*, 1179−1188.
15. Xu, Y., Mortimer, M. W., Fisher, T. S., Kahn, M. L., Brockman, F. J., and Xun, L. (1997) Cloning, sequencing and analysis of a gene cluster from *Chelatobacter heiztzii* ATCC 29600 encoding nitrilotriacetate monooxygenase and NADH:flavin mononucleotide oxidoreductase, *J. Bacteriol. 79*, 1112−1116.
16. Eichhorn, E., van der Ploeg, J. R., and Leisinger, T. (1999) Characterization of a two-component alkanesulfonate monooxygenase from *Escherichia coli*, *J. Biol. Chem. 274*, 26639−26646.
17. Hastings, J. W. (1996) Chemistries and colors of bioluminescent reactions: A review, *Gene 173*, 5−11.
18. Lei, B., and Tu, S.-C. (1998) Mechanism of reduced flavin transfer from *Vibrio harveyi* NADPH−FMN oxidoreductase to luciferase, *Biochemistry 37*, 14623−14629.
19. Kendrew, S. G., Harding, S. E., Hopwood, D. A., and Marsh, E. N. (1995) Identification of a flavin:NADH oxidoreductase involved in the biosynthesis of actinorhodin. Purification and characterization of the recombinant enzyme, *J. Biol. Chem. 270*, 17339−17343.
20. Valton, J., Filisetti, L., Fontecave, M., and Niviere, V. (2004) A two-component flavin-dependent monooxygenase involved in actinorhodin biosynthesis in *Streptomyces coelicolor*, *J. Biol. Chem. 279*, 44362−44369.
21. Thibaut, D., Ratet, N., Bisch, D., Faucher, D., Debussche, L., and Blanche, F. (1995) Purification of the two-enzyme system catalyzing the oxidation of the D-proline residue of pristinamycin IIB during the last step of pristinamycin IIA biosynthesis, *J. Bacteriol. 177*, 5199−5205.
22. Parry, R. J., and Li, W. (1997) Purification and characterization of isobutylamine *N*-hydroxylase from the valanimycin producer *Streptomyces viridifaciens* MG456-hF10, *Arch. Biochem. Biophys. 339*, 47−54.
23. Yeh, E., Garneau, S., and Walsh, C. T. (2005) Robust in vitro activity of RebF and RebH, a two-component reductase/halogenase, generating 7-chlorotryptophan during rebeccamycin biosynthesis, *Proc. Natl. Acad. Sci. U.S.A. 102*, 3960−3965.
24. Yeh, E., Cole, L. J., Barr, E. W., Bollinger, J. M., Jr., Ballou, D. P., and Walsh, C. T. (2006) Flavin redox chemistry precedes substrate chlorination during the reaction of the flavin-dependent halogenase RebH, *Biochemistry 45*, 7904−7912.

25. Arunachalam, U., Massey, V., and Miller, S. M. (1994) Mechanism of *p*-hydroxyphenylacetate-3-hydroxylase. A two-protein enzyme, *J. Biol. Chem. 269*, 150−155.
26. Arunachalam, U., and Massey, V. (1994) Studies on the oxidative half-reaction of *p*-hydroxyphenylacetate 3-hydroxylase, *J. Biol. Chem. 269*, 11795−11801.
27. Chakraborty, S., Ortiz-Maldonado, M., Eschenberg, K., Entsch, B., and Ballou, D. P. (2005) *p*-Hydroxyphenylacetate-3-hydroxylase from *Pseudomonas aeruginosa*, in *Flavins and Flavoproteins* (Nishino, T., Miura, R., Tanokura, M., and Fukui, K., Eds.) pp 275−280, ArchiTect, Inc., Tokyo, Japan.
28. Louie, T. M., Xie, X. S., and Xun, L. (2003) Coordinated production and utilization of $FADH_2$ by NAD(P)H−flavin oxidoreductase and 4-hydroxyphenylacetate 3-monooxygenase, *Biochemistry 42*, 7509−7517.
29. Thotsaporn, K., Sucharitakul, J., Wongratana, J., Suadee, C., and Chaiyen, P. (2004) Cloning and expression of *p*-hydroxyphenylacetate 3-hydroxylase from *Acinetobacter baumannii*: Evidence of the divergence of enzymes in the class of two-protein component aromatic hydroxylases, *Biochim. Biophys. Acta 1680*, 60−66.
30. Sucharitakul, J., Chaiyen, P., Entsch, B., and Ballou, D. P. (2005) The reductase of *p*-hydroxyphenylacetate 3-hydroxylase from *Acinetobacter baumannii* requires *p*-hydroxyphenylacetate for effective catalysis, *Biochemistry 44*, 10434−10442.
31. Sucharitakul, J., Chaiyen, P., Entsch, B., and Ballou, D. P. (2006) Kinetic mechanisms of the oxygenase from a two-component enzyme, *p*-hydroxyphenylacetate 3-hydroxylase from *Acinetobacter baumannii*, *J. Biol. Chem. 281*, 17044−17053.
32. Jeffers, C. E., Nichols, J. C., and Tu, S.-C. (2003) Complex formation between *Vibrio harveyi* luciferase and monomeric NADPH:FMN oxidoreductase, *Biochemistry 42*, 529−534.
33. Low. J. C., and Tu, S.-C. (2003) Energy transfer evidence for in vitro and in vivo complexes of *Vibrio harveyi* flavin reductase P and luciferase, *Photobiology 77*, 446−452.
34. Gao, B., and Ellis, H. R. (2005) Altered mechanism of the alkanesulfonate FMN reductase with the monooxygenase enzyme, *Biochem. Biophys. Res. Commun. 331*, 1137−1145.
35. Abdurachim, K., and Ellis, H. R. (2006) Detection of protein−protein interactions in the alkanesulfonate monooxygenase system from *Escherichia coli*, *J. Bacteriol. 188*, 8153−8159.
36. Duch, D. S., and Laskowski, M., Sr. (1971) A sensitive method for the determination of RNA in DNA and vice versa, *Anal. Biochem. 44*, 42−48.
37. Hazzard, J. T., Cusanovich, M. A., Tainer, J. A., Getzoff, E. D., and Tollin, G. (1986) Kinetic studies of reduction of a 1:1 cytochrome *c*−flavodoxin complex by free flavin semiquinones and rubredoxin, *Biochemistry 25*, 3318−3328.
38. Palfey, B. A., and Massey, V. (1998) Flavin-dependent enzyme, in *Comprehensive Biological Catalysis* (Michael, S., Ed.) Vol. 3, pp 83−153, Academic Press, San Diego, CA.
39. Entsch, B., Cole, L. J., and Ballou, D. P. (2005) Protein dynamics and electrostatics in the function of *p*-hydroxybenzoate hydroxylase. *Arch. Biochem. Biophys. 433*, 297−311.
40. Chaiyen, P., Brissette, P., Ballou, D. P., and Massey, V. (1997) Reaction of 2-methyl-3 hydroxypyridine-5-carboxylic acid (MHPC) oxygenase with *N*-methyl-5-hydroxynicotinic acid: Studies on the mode of binding, and protonation status of the substrate, *Biochemistry 36*, 13856−13864.
41. Chaiyen, P., Sucharitakul, J., Svasti, J., Entsch, B., Massey, V., and Ballou, D. P. (2004) Use of 8-substituted-FAD analogues to investigate the hydroxylation mechanism of the flavoprotein 2-methyl-3-hydroxypyridine-5-carboxylic acid oxygenase, *Biochemistry 43*, 3933−3943.
42. Lambeth, D. O., and Palmer, G. (1973) The kinetics and mechanism of reduction of electron transfer proteins and other compounds of biological interest by dithionite, *J. Biol. Chem. 248*, 6095−6103.
43. Ahmad, I., Cusanovich, M. A., and Tollin, G. (1981) Laser flash photolysis studies of electron transfer between semiquinone and fully reduced free flavins and horse heart cytochrome *c*, *Proc. Natl. Acad. Sci. U.S.A. 78*, 6724−6728.
44. Ahmad, I., Cusanovich, M. A., and Tollin, G. (1982) Laser flash photolysis studies of electron transfer between semiquinone and fully reduced free flavins and the cytochrome *c*−cytochrome oxidase complex, *Biochemistry 22*, 3122−3128.
45. Alfieri, A., Fersini, F., Ruangchan, N., Prongjit, M., Chaiyen, P., and Mattevi, A. (2007) Structure of the monooxygenase component of a two-component flavoprotein monooxygenase, *Proc. Natl. Acad. Sci. U.S.A. 104*, 1177−1182.
46. Bruice, T. C. (1984) Oxygen−flavin chemistry, *Isr. J. Chem. 24*, 54−61.
47. Massey, V., Strickland, S., Mayhew, S. G., Howell, L. G., Engel, P. C., Matthews, R. G., Schuman, M., and Sullivan, P. A. (1969) The production of superoxide anion radicals in the reaction of reduced flavins and flavoproteins with molecular oxygen, *Biochem. Biophys. Res. Commun. 36*, 891−897.
48. Massey, V., Palmer, G., and Ballou, D. P. (1971) On the reaction of reduced flavins and flavoproteins with molecular oxygen, in *Flavins and Flavoproteins*, 3rd International Symposium (Kamin, H., Ed.) pp 349−361, University Park Press, Baltimore, MD.
49. Tu, S.-C. (2001) Reduced flavin: Donor and acceptor enzymes and mechanisms of channeling, *Antioxid. Redox Signaling 3*, 881−897.

BI7006614